Importance of Specific Nucleotides in the Folding of the Natural Form of the Hairpin Ribozyme†

Timothy J. Wilson, Zheng-Yun Zhao, Kaera Maxwell, Loucas Kontogiannis, and David M. J. Lilley*

CRC Nucleic Acid Structure Research Group, Department of Biochemistry, The University of Dundee, Dundee DD1 4HN, U.K.

Received November 16, 2000; Revised Manuscript Received December 15, 2000

ABSTRACT: The hairpin ribozyme in its natural context consists of two loops in RNA duplexes that are connected as arms of a four-way helical junction. Magnesium ions induce folding into the active conformation in which the two loops are in proximity. In this study, we have investigated nucleotides that are important to this folding process. We have analyzed the folding in terms of the cooperativity and apparent affinity for magnesium ions as a function of changes in base sequence and functional groups, using fluorescence resonance energy transfer. Our results suggest that the interaction between the loops is the sum of a number of component interactions. Some sequence variants such as A10U, G+1A, and C25U exhibit loss of cooperativity and reduced affinity of apparent magnesium ion binding. These variants are also very impaired in ribozyme cleavage activity. Nucleotides A10, G+1, and C25 thus appear to be essential in creating the conformational environment necessary for ion binding. The double variant G+1A/C25U exhibits a marked recovery of both folding and catalytic activity compared to either individual variant, consistent with the proposal of a triple-base interaction among A9, G+1, and C25 [Pinard, R., Lambert, D., Walter, N. G., Heckman, J. E., Major, F., and Burke, J. M. (1999) *Biochemistry 38*, 16035−16039]. However, substitution of A9 leads to relatively small changes in folding properties and cleavage activity, and the double variant G+1DAP/C25U (DAP is 2,6-diaminopurine), which could form an isosteric triple-base interaction, exhibits folding and cleavage activities that are both very impaired compared to those of the natural sequence. Our results indicate an important role for a Watson−Crick base pair between G+1 and C25; this may be buttressed by an interaction with A9, but the loss of this has less significant consequences for folding. 2′-Deoxyribose substitution leads to folding with reduced magnesium ion affinity in the following order: unmodified RNA > dA9 > dA10 > dC25 ∼ dA10 plus dC25. The results are interpreted in terms of an interaction between the ribose ring of C25 and the ribose and base of A10, in agreement with the proposal of Ryder and Strobel [Ryder, S. P., and Strobel, S. A. (1999) *J. Mol. Biol. 291*, 295−311]. In general, there is a correlation between the ability to undergo ion-induced folding and the rate of ribozyme cleavage. An exception to this is provided by G8, for which substitution with uridine leads to severe impairment of cleavage but folding characteristics that are virtually unaltered from those of the natural species. This is consistent with a direct role for the nucleobase of G8 in the chemistry of cleavage.

RNA catalysis occurs in nature in the cleavage and ligation of RNA species mediated by the small nucleolytic ribozymes (*1*, *2*), in RNA splicing by group I (*3*) and II introns (*4*), and in the peptidyl transferase activity of the ribosome (*5*). Ribozymes may also offer a glimpse into a postulated earlier phase in the evolution of life on the planet, in which RNA was both the primary informational and catalytic species (*6*, *7*). Despite its importance, however, the origins of catalytic activity in RNA molecules is still imperfectly understood. While the central role played by RNA folding is beyond dispute, the relative importance of participation of metal ions and nucleobases and the role of local RNA conformation have still not been fully determined (*1*).

The nucleolytic ribozymes provide a useful source of information about RNA catalysis because of their small size and relative simplicity. The hairpin ribozyme (*8*) is a self-processing element that exists in the negative strand of the satellite RNA of the tobacco ringspot virus (*9*−*11*) and similar plant viruses (*12*). The ribozyme facilitates the processing of concatameric RNA resulting from rolling-circle replication, as well as the reverse ligation reaction (*9*), generating circular monomeric RNA (*13*). The ability of the ribozyme to catalyze both cleavage and ligation leads to an equilibrium (*14*).

The hairpin ribozyme is constructed from two loop-bearing duplexes that exist as adjacent arms of a four-way junction (Figure 1). The majority of essential bases (*15*−*17*) and functional groups (*18*−*20*) are located in these loops, and cleavage activity was found to be retained when the loop-carrying arms were connected together in a variety of ways (*21*−*26*). Some activity was even observed in trans with unconnected loop-carrying duplexes (*22*, *27*). This led to the expectation that close interaction between the loops would be required to generate the active form of the ribozyme, which was supported by chemical cross-linking studies (*26*).

† We thank the CRC and BBSRC for financial support.

* To whom correspondence should be addressed. Telephone: (44)-1382-344243. Fax: (44)-1382-201063. E-mail: dmjlilley@bad.dundee.ac.uk.

10.1021/bi002644p CCC: $20.00
Published on Web 01/26/2001

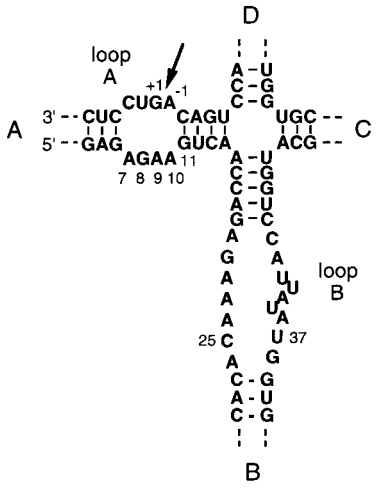

FIGURE 1: The hairpin ribozyme. The base sequence of tobacco ringspot virus satellite (−) RNA around the hairpin ribozyme (*11*), with the site of cleavage denoted with an arrow. The four helical arms are labeled A and B (containing the loops A and B, respectively), with C and D continuing in a circular manner. Specific nucleotides mentioned in the text are identified by numbering (*32*). The complete sequences of the species used in the experiments in these studies can be obtained from Materials and Methods.

Physical evidence for this was obtained using fluorescence resonance energy transfer (FRET),[1] showing the close approach of the ends of the two loop-carrying duplex arms (*28*−*30*).

Folding of the hairpin ribozyme by close association of the loops is induced by divalent metal ions, in the absence of which there is no detectable interaction. Although the ribozyme functions if the junction is replaced with a simple hinge point (*11*, *31*, *32*), the folding is very much less efficient than that of the natural ribozyme in its context of a four-way helical junction. The natural species is induced to fold by the cooperative binding of magnesium ions in the concentration range of 30−50 μM (*29*), whereas the hinged form requires an almost 1000-fold higher concentration of ions (*33*). The greater efficiency of folding of the junction form has also been shown by time-resolved FRET measurements (*34*). The product complex is more stable in this form (*35*), shifting the equilibrium toward the ligation reaction.

Ion-induced folding of the natural form of the ribozyme involves the combined participation of loops A and B and the four-way helical junction which brings about a close association of the loops. Their interaction presumably creates the local environment at the scissile phosphate required to accelerate the transesterification reaction that leads to either breakage or religation of the RNA backbone. The interaction is likely to involve a number of specific contacts between nucleotides in both loops, and probably some structural reorganization within both loops. One approach to identifying these contacts is to search for changes in sequence or functional groups that alter the folding process, and perhaps further changes that lead to in vitro complementation and restoration of normal folding. We have previously identified a number of sequence variants of the hammerhead ribozyme that exhibit perturbed folding (*36*, *37*), and these have been very useful in the dissection of the ion-induced folding process for that species (*38*). One clear example of a folding variant of the hairpin ribozyme is the G+1A species. This is severely impaired in cleavage activity in both the hinged (*32*) and junction forms (*33*) of the ribozyme, and ion-induced folding is compromised in both forms (*30*, *33*). In the study presented here, we have analyzed the folding of variant hairpin ribozyme species in the natural junction form as a function of changes of local sequence and functional groups. Our results suggest that the interaction between the loops is the sum of a number of component interactions, and we identify nucleotides involved in these interactions. In general, we find a correlation between the ability to undergo ion-induced folding and the rate of ribozyme cleavage. A marked exception to this is provided by G8, mutation of which leads to severe impairment of cleavage but virtually unaltered folding characteristics. While we are open to alternative explanations, this would be consistent with a direct role for the nucleobase of G8 in the chemistry of cleavage.

MATERIALS AND METHODS

Chemical Synthesis of RNA-Containing Oligonucleotides. Oligonucleotides were synthesized using phosphoramidite chemistry (*59*) implemented on an Applied Biosystems 394 DNA/RNA synthesizer. RNA was synthesized using ribonucleotide phosphoramidites with 2′-*O*-*tert*-butyldimethylsilyl (*t*-BDMS) protection (*60*, *61*) (ProOligo). 2′-Deoxyribonucleosides were introduced at positions indicated in the text. 2,6-Diaminopurine was coupled with 2′-*O*-triisopropylsilyloxymethyl protection (Glen Research), while 2-aminopurine was coupled as a 2′-deoxyribonucleoside. Fluorescein (PE-ABI) and indocarbocyanine-3 (Cy3, Glen Research) were coupled to the 5′-termini as phosphoramidites. Oligoribonucleotides were deprotected in a 25% ethanol/ammonia solution at 55 °C for 6 h (fluorophore-labeled) or 12 h (unlabeled) and evaporated to dryness. Oligoribonucleotides were redissolved in 0.5 mL of 1 M tetrabutylammonium fluoride (Aldrich) in tetrahydrofuran to remove *t*-BDMS groups, and agitated at 20 °C in the dark for 16 h prior to desalting by G25 Sephadex (NAP columns, Pharmacia) and ethanol precipitation. Fully deprotected oligonucleotides were purified by gel electrophoresis in 20% polyacrylamide containing 7 M urea. Bands were excised, and the oligonucleotides were electroeluted into 8 M ammonium acetate, and recovered by ethanol precipitation. Fluorescently labeled oligonucleotides were further purified by reversed-phase HPLC. Samples were dissolved in 100 mM ammonium acetate (pH 7.5) and applied to a C18 reversed-phase column (μ Bondapak, Waters). RNA was eluted with a linear gradient of acetonitrile and 100 mM ammonium acetate (pH 7.5) with a flow rate of 1 mL/min. The peak fractions were evaporated to dryness, redissolved in water, and ethanol precipitated.

Transcription of RNA. RNA was transcribed from synthetic DNA templates using T7 RNA polymerase according to the method described in ref *62*, and purified by polyacrylamide gel electrophoresis.

Analysis of Ribozyme Cleavage. Ribozyme and 5′-^{32}P-labeled substrate were individually incubated in 50 mM Tris-HCl (pH 7.5) at 90 °C for 2 min, followed by 15 min at the indicated temperature. Magnesium chloride was added to a

[1] Abbreviations: DAP, 2,6-diaminopurine; AP, 2-aminopurine; FRET, fluorescence resonance energy transfer; NMR, nuclear magnetic resonance; HDV, hepatitis delta virus; *t*-BDMS, 2′-*O*-*tert*-butyldimethylsilyl; HPLC, high-pressure liquid chromatography.

final concentration of 10 mM, and incubation continued for a further 60 min. The reaction was initiated by mixing the ribozyme and substrate at final concentrations of 1 μM and 50 nM, respectively. The cleavage reactions were stopped at the indicated times, and product formation was analyzed by electrophoresis on sequencing gels containing 7 M urea. Product formation was quantified by exposure to storage phosphor screens and phosphorimaging (BAS-1500, Fuji). Progress curves [fraction of uncleaved substrate (*f*) as a function of time] were fitted to a single-exponential function:

$$f = e^{-k_{obs}t} \quad (1)$$

where t is the time of incubation and k_{obs} the observed rate constant. Experimental errors were determined from reactions performed in triplicate. In general, the errors are less than 10% of the measured rates. Substrate strands were chemically synthesized, based on the natural sequence (all sequences written 5′ to 3′, with deoxyribonucleotides underscored; UUCGGCCACCUGACAGUCCUG). Variants were synthesized with A or DAP at the +1 position. The ribozyme strands were prepared by transcription, based on the natural sequence (GGCCACAGAGAAGUCAACCAGAGAAACACACGUUGUGGUAUAUUACCUGGUACGCCGAAAGGCGUGGUGGCCGAA). Variants were prepared with the single-base changes A7U, G8U, A9U, A10U, and C25U.

Construction of Hairpin Ribozyme Species for FRET Analysis. Fluorescent hairpin species for FRET studies were constructed by incubation of a mixture of stoichiometric quantities of one fluorescein-labeled strand, one Cy3-labeled strand, and two unlabeled strands in 90 mM Tris-borate (pH 8.3) and 25 mM NaCl for 10 min at 80 °C, followed by slow cooling. The hybridized species were purified by electrophoresis in a 10% polyacrylamide gel at 4 °C for 20 h at 120 V. The buffer system contained 90 mM Tris-borate (pH 8.3) and 25 mM NaCl and was recirculated at a rate of >1 L/h. Fluorescent junctions were visualized by illumination using a Dark Reader transilluminator (Clare Chemical Research); the bands were excised, and the RNA was electroeluted into 8 M ammonium acetate and recovered by ethanol precipitation. FRET analysis of the various forms of the hairpin ribozyme employed synthetic RNA species (with 5′-fluorophores where appropriate) of the following sequences (all written 5′ to 3′, with deoxyribonucleotides underscored): a strand, CCGCACAGAGAAGUCAACCAGAGAAACACACCGG; b strand, CCGGUGGUAUAUUACCUGGUACGCCUUGACGUGGGGG; c strand, CCCCACGUCAAGGCGUGGUGGCCGAAGGUCGG; and d strand, CCGACCUUCGGCCACCUGACAGUCCUGUGCGG. Modified versions of the a strand were synthesized containing the A7U, G8U, A9U, A10U, or C25U base substitution, and the single-2′-deoxyribose substitution at A9, A10, or C25, or the double substitution at A10 and C25. Modified d strand species containing A, DAP, or AP at the +1 position were synthesized.

Fluorescence Spectroscopy. Fluorescence spectra were recorded at 4 °C using an SLM-Aminco 8100 fluorimeter, in 90 mM Tris-borate (pH 8.3). Spectra were corrected for lamp fluctuations and instrumental variations, as described in ref *38*. Polarization artifacts were avoided by setting excitation and emission polarizers crossed at 54.74°. Values of E_{FRET} were measured using the acceptor normalization method (*42*, *63*) in which an extracted acceptor spectrum $F^A(\nu_1,\nu')$ (excitation at $\nu' = 490$ nm, emission at ν_1) is normalized to a second spectrum $[F(\nu_2,\nu'')]$ from the same sample excited at a wavelength ($\nu'' = 547$ nm) at which only the acceptor is excited, with emission at ν_2. This gives the acceptor ratio

$$(\text{ratio})_A = F^A(\nu_1,\nu')/F(\nu_2,\nu'') = \{E_{FRET}d^+[\epsilon^D(\nu')/\epsilon^A(\nu'')] + [\epsilon^A(\nu')/\epsilon^A(\nu'')]\}[\Phi^A(\nu_1)/\Phi^A(\nu_2)] \quad (2)$$

Superscripts D and A refer to donor and acceptor, respectively. ϵ^D and ϵ^A are the molar absorption coefficients at the indicated frequency of the donor and acceptor, respectively, and Φ^A is the fluorescent quantum yield of the acceptor. d^+ is the molar fraction of the species labeled with the donor fluorophore. E_{FRET} may be calculated from $(\text{ratio})_A$ since $\epsilon^D(\nu')/\epsilon^A(\nu'')$ and $\epsilon^A(\nu')/\epsilon^A(\nu'')$ are measured from absorption spectra, and $\Phi^A(\nu_1)/\Phi^A(\nu_2)$ is unity when $\nu_1 = \nu_2$.

Analysis of Fluorescence Data. Data from magnesium ion titrations were analyzed on the assumption of a simple two-state model for ion-induced folding:

$$RNA_{unfolded} + xMg^{2+} \rightleftharpoons RNA_{folded}\cdot Mg^{2+}_x$$

whereby the change in FRET efficiency on magnesium ion binding (ΔE_{FRET}) is given by

$$\Delta E_{FRET} = \alpha[E_{FRET}(\text{folded}) - E_{FRET}(\text{unfolded})] \quad (3)$$

where α is the fraction of molecules in the folded state, given by

$$\alpha = K_A[Mg^{2+}]^n/(1 + K_A[Mg^{2+}]^n) \quad (4)$$

where K_A is the apparent association constant for magnesium ions and n is a Hill coefficient. Data were fitted to this equation by nonlinear regression. Errors reported for n are the asymptotic standard errors on the fits. The magnesium ion concentration at which the transition is half-complete ($[Mg^{2+}]_{1/2}$) is given by $(1/K_A)^{1/n}$. In duplicate experiments, the Hill coefficients agreed to within 0.2, and $[Mg^{2+}]_{1/2}$ values to within 10%.

RESULTS

Role of Loop A in the Folding of the Hairpin Ribozyme

We have made a systematic study of the folding of the hairpin ribozyme in its natural junction form, as a function of the sequence of the nonsubstrate strand of loop A. We have analyzed the cleavage activity and ion-induced folding of species in which each of the four purine bases has been individually replaced with uridine. The results of these studies are collected together in Table 1.

Effect of Sequence Changes in Loop A on Hairpin Ribozyme Activity. We have analyzed the cleavage activity of the hairpin ribozyme as a function of base substitution in loop A. For this purpose, we employed a two-stranded construct, comprising a transcribed ribozyme strand together with a chemically synthesized radioactively 5′-^{32}P-labeled

Table 1: Folding and Cleavage Characteristics of the Natural-Sequence Hairpin Ribozyme in the Junction Form, and Single-Base Sequence Variants in Loop A[a]

sequence variant	cleavage rate (min^{-1})	FRET vector	Hill coefficient n	$[Mg^{2+}]_{1/2}$ (μM)
natural	4.6×10^{-2}	BA	2.0 ± 0.1	30
A7U	4.0×10^{-2}	BA	2.4 ± 0.1	76
		DC	2.3 ± 0.1	69
G8U	4.2×10^{-4}	BA	2.1 ± 0.3	46
		DC	2.1 ± 0.4	47
A9U	1.6×10^{-2}	BA	2.0 ± 0.1	125
		DC	1.9 ± 0.2	105
A10U	7.2×10^{-3}	BA	0.9 ± 0.1	640
		DC	1.2 ± 0.1	700
G+1A	4.2×10^{-5}	BA	1.0 ± 0.1	650
junction	−	BA	1.1 ± 0.2	2500

[a] Folding data are presented for FRET analysis of both BA and DC vectors. Hill coefficients and $[Mg^{2+}]_{1/2}$ values were derived by fitting FRET efficiencies for end-to-end vectors to a two-state folding model. The errors reported for the Hill coefficients are the asymptotic standard errors. Cleavage rate constants are the mean of three determinations of cleavage rates under single-turnover conditions at 25 °C. Data for the G+1A variant (*33*) and for the simple junction (*64*) have been included for comparison.

substrate strand (Figure 2A). In this species, the junction-distal helix of arm A can only form three base pairs (*33*), and thus, the product to the 3′-side of the cleavage should readily diffuse away, reducing the probability of religation.

Analysis of the product after a 10 min incubation with magnesium ions at 25 °C (Figure 2B) shows that there are significant differences in sensitivity to base substitution at the different positions. The amount of product from the A7U variant is similar to that of the natural-sequence ribozyme; this is consistent with earlier studies (*15*, *39*), where it has been observed that the hinged form of the ribozyme is relatively insensitive to changes in sequence at this position. By contrast, uridine substitution at positions 9 and 10 led to a marked reduction in the level of product, while the G8U substitution results in undetectable cleavage after 10 min. Reaction rates were measured from time courses performed in triplicate, and the reaction progress is plotted in Figure 2C. The calculated first-order rate constants are listed in Table 1. The rates show that the order of cleavage rates for the ribozymes in the junction form is as follows: natural ≥ A7U > A9U > A10U > G8U. Although the rate of cleavage by the G8U hairpin species is low, significant ribozyme activity can be detected by extending the time course as shown in Figure 2D.

Effect of Sequence Changes in Loop A on Ion-Induced Folding of the Hairpin Ribozyme. We have studied the folding of the hairpin ribozyme by fluorescence resonance energy transfer between donor and acceptor fluorophores attached to the 5′-termini of selected helical arms as in our previous investigations (*28*, *29*, *40*). The efficiency of energy transfer (E_{FRET}) between donor and acceptor fluorophore pairs attached to the ends of different pairs of arms depends inversely on the separation between the fluorophores (R) according to (*41*)

$$E_{FRET} = 1/[1 + (R/R_0)^6] \quad (5)$$

where R_0 is the characteristic distance at which $E_{FRET} = 0.5$. Thus, the relative distances for different end-to-end vectors of the four-way junction can be compared, as well as the

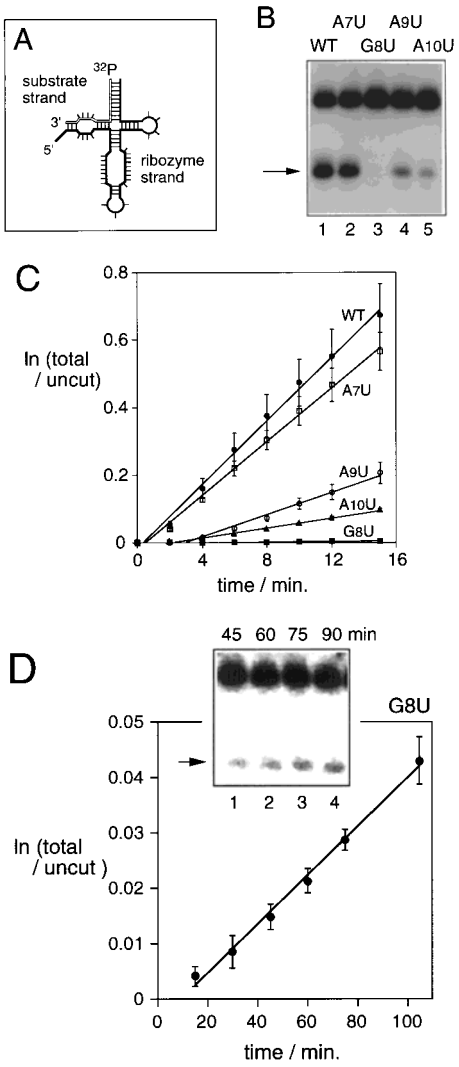

FIGURE 2: Cleavage activity of the hairpin ribozyme, and single-base variants modified in loop A. (A) Scheme showing the construct used to examine cleavage activity of the junction form of the ribozyme. It consists of two strands, a ribozyme strand (black) and a radioactively 5′-^{32}P-labeled substrate strand (open). (B) Comparison of ribozyme cleavage of the natural sequence and loop A variants. Ribozyme and radioactively labeled substrate strands were incubated in the presence of 10 mM magnesium ions at 25 °C for 10 min. The reaction was terminated, and the substrate and product were separated by electrophoresis in polyacrylamide and visualized by exposure to X-ray film. The resulting autoradiograph is shown. The product band is denoted with an arrow: lane 1, natural-sequence ribozyme; lane 2, A7U variant; lane 3, G8U variant; lane 4, A9U variant; and lane 5, A10U variant. (C) Progress of the cleavage reaction. Ribozyme and radioactively labeled substrate strands (natural sequence and variants) were incubated in the presence of 10 mM magnesium ions at 25 °C, and aliquots were removed at various times. Products were separated by polyacrylamide gel electrophoresis and quantified by phosphorimaging. The data are plotted in semilogarithmic form, from which rate constants were calculated. The data points are averages of triplicate measurements, and the errors are standard deviations: (●) natural sequence, (□) A7U, (○) A9U, (▲) A10U, and (■) G8U. (D) Ribozyme activity of the G8U hairpin species. To observe the cleavage activity of this variant, a more extended time course was used. The ribozyme and radioactively labeled substrate strand were incubated in the presence of 10 mM magnesium ions at 25 °C in triplicate as before. The plot shows reaction progress over the course of 105 min in semilogarithmic form. Data points are averages, and the errors are standard deviations. The inset shows a phosphorimage of the reaction product (denoted with an arrow) as a function of time: lane 1, 45 min; lane 2, 60 min; lane 3, 75 min; and lane 4, 90 min.

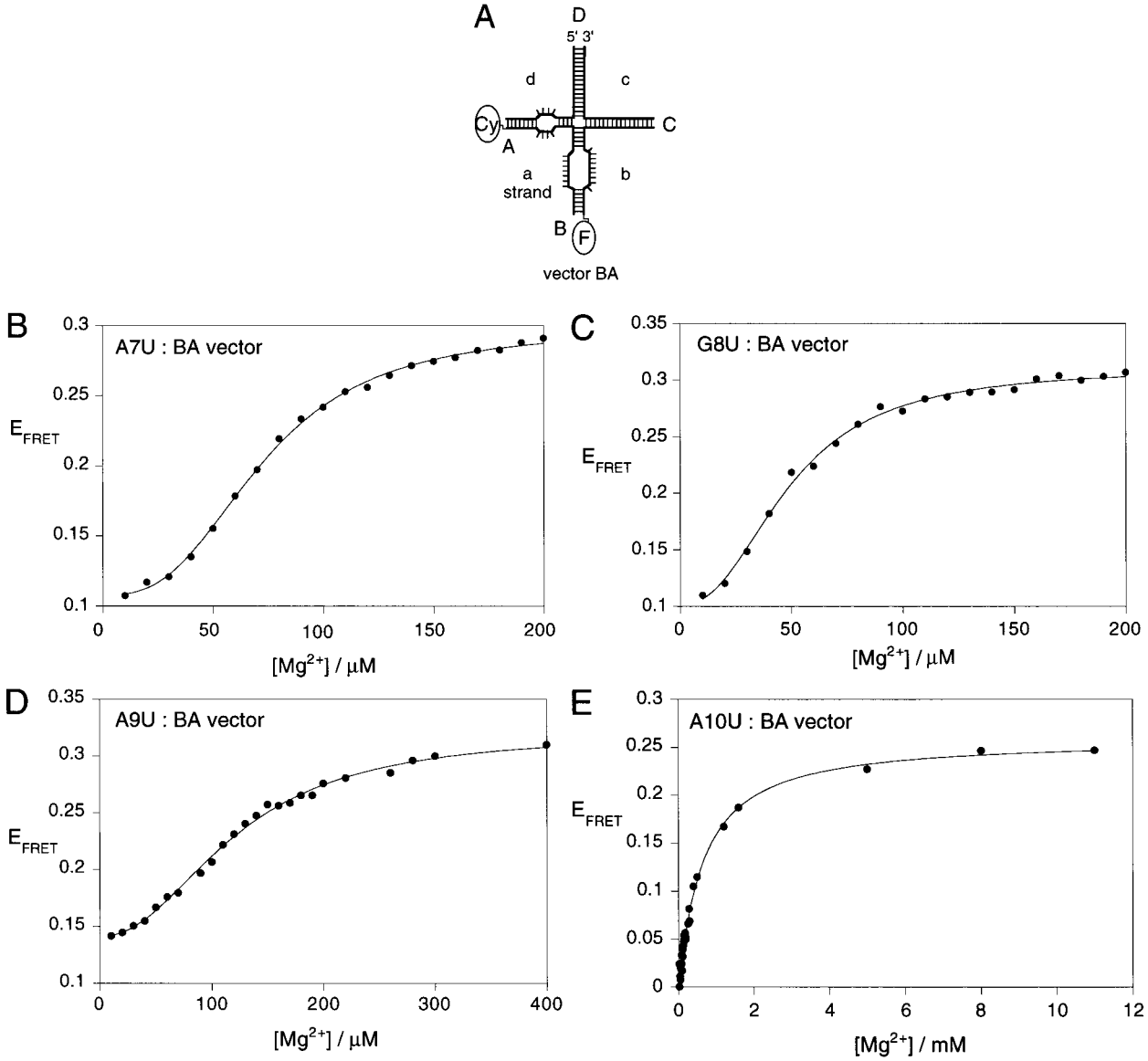

FIGURE 3: Magnesium ion-induced folding of the hairpin ribozyme single-base variants modified in loop A. (A) Folding has been analyzed by FRET, using species with terminally attached fluorophores. The vectors are named according to the arms carrying donor (fluorescein, F) and acceptor (Cy3, Cy) fluorophores in that order. The BA species is illustrated. (B−E) FRET efficiencies (E_{FRET}) (●) as a function of magnesium ion concentration were fitted by regression to a two-state folding model. The lines show the fits to the model for the BA species, from which the values of apparent association constants and Hill coefficients have been calculated. (B) Folding of the A7U hairpin ribozyme over the magnesium ion concentration range of 0−200 μM. (C) Folding of the G8U hairpin ribozyme over the magnesium ion concentration range of 0−200 μM. (D) Folding of the A9U hairpin ribozyme over the magnesium ion concentration range of 0−400 μM. (E) Folding of the A10U hairpin ribozyme over the magnesium ion concentration range of 0−11 mM. Note the different shape of the magnesium ion dependence of folding for this species, indicative of noncooperative behavior.

change in length of given vectors as the molecule undergoes ion-induced folding. Since our experiments employ species with four arms of near-equal length, these end-to-end distances reflect the different angles subtended between the different pairs of helical arms, though the nonstandard helical geometry of the loops complicates this estimation. Each helix in the hairpin constructs terminated in a 5′-CC sequence; we have previously found that this provides a well-behaved environment for FRET measurements in nucleic acids (*42*−*45*). For a given vector, a junction will comprise one strand labeled with fluorescein, one labeled with Cy3, and two unlabeled strands (Figure 3A). All species used in FRET experiments contain a 2′-deoxyribose substitution at A−1 for prevention of ribozyme cleavage during the experiment. We have recently shown that removal of the catalytic hydroxyl does not significantly alter the folding properties of the molecule (*33*).

There are six different end-to-end distances that can be studied, although two are particularly informative. Species where the fluorophores are attached to the ends of helices A and B, or to helices C and D, exhibit the greatest change in FRET efficiency since they are the shortest distances in the folded structure. For the majority of these studies, we have concentrated on the shortening of the BA vector, i.e., the species in which helices B and A carry fluorescein and cyanine-3 (Cy3), respectively.

Effect of the A7U Sequence Change on Folding. Energy transfer efficiencies were measured for six end-to-end species of the A7U hairpin ribozyme in the presence of different magnesium ion concentrations. At low magnesium ion

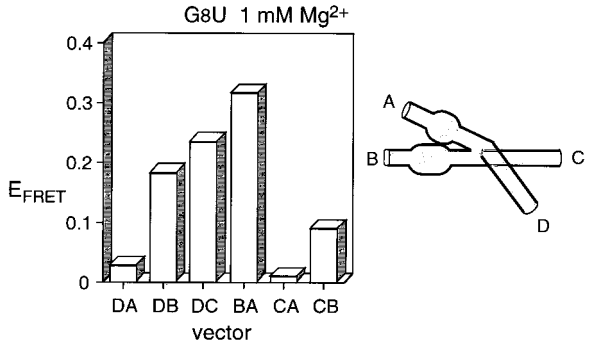

FIGURE 4: Global shape of the junction form of the G8U hairpin ribozyme deduced from FRET measurements. Histogram of the FRET efficiencies for six end-to-end vectors measured in the presence of 1 mM magnesium ions. The observed pattern of efficiencies is closely similar to that observed previously for the junction form of the ribozyme with an unmodified sequence (*28*). The shortest interfluorophore distance is observed for the BA vector. The pattern is consistent with the formation of the folded structure illustrated on the right.

concentrations, the values of E_{FRET} are low (<0.10) for all species, consistent with an extended structure. On addition of magnesium ions, we observed a marked change in the pattern of efficiencies. The BA species reaches an E_{FRET} of 0.3, and there is an order of efficiencies described as follows: BA > DC > DB > CB, DA, and CA (data not shown). This is closely similar to the set of efficiencies obtained using the natural sequence (*28*, *29*), and indicates that the structure formed in magnesium ions is closely similar to that of the unmodified ribozyme. Further information about the ion-induced folding can be obtained by a more detailed titration of one of the vectors that exhibits marked shortening. Figure 3B shows the FRET efficiency for the BA vector over the magnesium ion concentration range of 0−200 μM. These data have been fitted using a two-state model (see Materials and Methods), giving the apparent association constant for magnesium ions (K_A) and a Hill coefficient (n). From this, we can calculate the magnesium ion concentration at which the transition is half-complete ($[Mg^{2+}]_{1/2}$), given by $(1/K_A)^{1/n}$. The profile of E_{FRET} as a function of magnesium ion concentration has a shape that indicates that the transition is induced by cooperative ion binding, and the Hill coefficient n of 2.4 ± 0.1 confirms this. The $[Mg^{2+}]_{1/2}$ value of 76 μM is a little higher than that of the unmodified hairpin ribozyme. Closely similar values were obtained by studying the DC vector, where we follow the approach of the two remaining arms of the ribozyme that do not carry the loops. Overall, the folding characteristics of the A7U hairpin are very similar to those of the unmodified ribozyme.

Effect of the G8U Sequence Change on Folding. The ion-induced folding of the G8U hairpin is even closer to that of the natural-sequence ribozyme. The pattern of FRET efficiencies of six end-to-end vectors in the presence of 1 mM magnesium ions is shown in Figure 4; it is closely similar to those obtained previously for the species with the natural sequence. The profiles of E_{FRET} as a function of magnesium ion concentration for the BA (Figure 3C) and DC vectors are typical of those indicating cooperative ion binding, and values of the Hill coefficient calculated from fits to the two-state folding model were within experimental error of 2.0 (Table 1). The half-magnesium ion concentrations (46 and 47 μM) indicate that the folding of this variant is induced by ion binding with an affinity very similar to that of the unmodified hairpin ribozyme.

Effect of the A9U Sequence Change on Folding. The A9U hairpin was found to exhibit mildly impaired folding in response to addition of magnesium ions. The eventual folded structure was closely similar to that of the unmodified species, indicated by the FRET efficiencies of the six end-to-end vectors (data not shown), and the folding remained cooperative, with Hill coefficients of ~2.0 for both the BA (Figure 3D) and DC vectors (Table 1). However, the folding occurred at a somewhat higher magnesium ion concentration, indicating a reduced affinity for the transition-inducing magnesium ions. This effect was not large, and the folding overall remains quite similar to that of the natural-sequence ribozyme.

Effect of the A10U Sequence Change on Folding. In contrast to the other variants, the A10U hairpin ribozyme has markedly perturbed folding characteristics. The magnesium ion-dependent folding isotherm (Figure 3E) has a shape associated with noncooperative binding, and values of the Hill coefficient of unity (within experimental error) were obtained for both BA and DC vectors (Table 1). The affinity for the magnesium ions causing the transition to the folded structure was much lower, with half-magnesium ion concentrations of approximately 650 μM. The folding of the A10U hairpin is severely compromised, with characteristics close to those previously noted for the G+1A variant (*33*).

Investigation of the Potential Ribose Zipper on Folding

Burke and co-workers (*18*) showed that there are relatively few positions in the hairpin ribozyme at which removal of the 2′-hydroxyl group had a major effect on the cleavage rate in the hinged form, A10, G11, A24, and C25 being the positions most sensitive to this modification. This was later confirmed by detailed nucleotide analogue interference mapping experiments (*46*). Gait and colleagues (*26*) proposed the existence of a ribose zipper (*47*) linking the backbones of loops A and B by hydrogen bonding between A10 and C25, and between G11 and A24. The proposal was revised in light of further functional group substitution experiments (*46*, *48*), but retained an interaction between the ribose groups of A10 and C25.

All the investigations of the importance of 2′-hydroxyl groups to date have been restricted to analysis of their effect on the cleavage activity of the ribozyme. While it might be expected that reduction in cleavage rates would be a consequence of impaired folding, this has not been explicitly investigated in either the hinged or junction form of the RNA. We have therefore used FRET to analyze the ion-induced folding of the ribozyme in its natural junction form, as a function of the removal of selected 2′-OH groups. In these experiments, we have studied the efficiency of energy transfer between the termini of the A and B arms. Each variant has been titrated with magnesium ions, and the data over the range of 0−800 μM fitted to a two-state model as before. The results are presented in Figure 5 and summarized in Table 2.

Removal of the 2′-hydroxyl at A9 in loop A has a small effect on folding. The Hill coefficient is 2.0 ± 0.3, but the apparent affinity for magnesium ions is slightly reduced from that of the unmodified sequence ($[Mg^{2+}]_{1/2}$ = 99 μM,

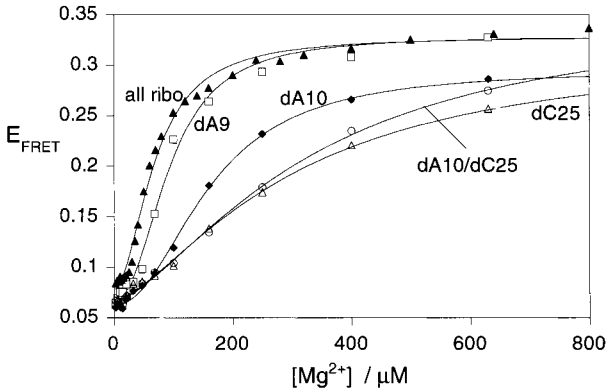

FIGURE 5: Ion-induced folding of 2′-deoxyribose-substituted hairpin ribozyme variants. Plot of FRET efficiency as a function of magnesium ion concentration in the range of 0−800 μM for the BA vectors of the unmodified ribozyme (▲), three singly deoxyribose-substituted species [dA9 (□), dA10 (◆), and dC25 (△)] and one doubly substituted species [dA10/dC25 (○)]. Each of these data sets has been fitted by regression to the two-state model (lines).

Table 2: Folding Characteristics of 2′-Deoxyribose-Substituted Variants of the Hairpin Ribozyme in Its Junction Form[a]

2′-H position	Hill coefficient *n*	$[Mg^{2+}]_{1/2}$ (μM)
A9	2.0 ± 0.3	99
A10	2.1 ± 0.1	160
C25	1.4 ± 0.1	320
A10 plus C25	1.5 ± 0.1	320

[a] Hill coefficients and $[Mg^{2+}]_{1/2}$ values were derived by fitting FRET efficiencies for end-to-end vectors to a two-state folding model. The errors reported for the Hill coefficients are the asymptotic standard errors.

compared to <50 μM for the natural sequence). 2′-Hydroxyl modification of the adjacent A10 has a larger effect, reducing the apparent magnesium ion affinity to a $[Mg^{2+}]_{1/2}$ of 160 μM while leaving the Hill coefficient essentially unaltered at 2.1 ± 0.1. The largest effect resulting from the removal of a single 2′-hydroxyl was observed at C25, where a lowering of cooperativity (n = 1.4 ± 0.1) and a significant reduction in apparent affinity for magnesium ions ($[Mg^{2+}]_{1/2}$ = 320 μM) were observed. When the 2′-hydroxyl groups of both A10 and C25 were simultaneously absent, closely similar values for n and $[Mg^{2+}]_{1/2}$ of 1.5 ± 0.1 and 320 μM, respectively, were measured. The set of variants can be ranked in order of the apparent affinity for magnesium ions: natural > A9 > A10 > C25 ∼ A10/C25. We have not examined the cleavage activity of these variants, but we note that the rank order is fully consistent with the cleavage rates measured by Earnshaw et al. (*48*) in the context of the hinged ribozyme. The folding of none of the variants is impaired to the degree of the isolated junction, or the G+1A or A10U sequence variants, and cooperative magnesium ion binding is retained, although its level is reduced for the C25 variant.

Investigation of a Potential Triple-Base Interaction on Folding and Activity

We have shown above that the A9U variant of the hairpin ribozyme in its junction form is partially impaired in folding and cleavage activity. Burke and colleagues (*32*) have found that the G+1A sequence change results in the loss of activity of the ribozyme in the hinged form, and we have recently shown that in the junction form the G+1A ribozyme is

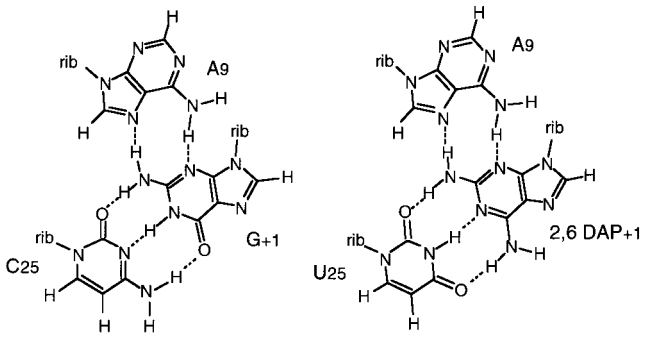

FIGURE 6: Proposed triple-base interaction. The proposed triple-base interaction between A9, G+1, and C25 (*50*) is shown on the left. It consists of a conventional Watson−Crick base pair between C25 and G+1, and an interaction between the major groove face of A9 and the minor groove face of G+1. An isosteric triple-base interaction can be written with the double substitution C25U/G+1DAP (2,6-diaminopurine), shown at the right.

Table 3: Folding and Cleavage Characteristics of G+1 and C25 Variants of the Hairpin Ribozyme in Its Junction Form[a]

position +1 base	position 25 base	cleavage rate (min^{-1})	Hill coefficient *n*	$[Mg^{2+}]_{1/2}$ (μM)
G	C	4.6×10^{-2}	2.0 ± 0.1	30
G	U	2.0×10^{-4}	0.9 ± 0.04	940
A	C	4.2×10^{-5}	1.0 ± 0.1	650
A	U	5.3×10^{-3}	2.1 ± 0.2	430
DAP	C	1.9×10^{-4}	1.1 ± 0.04	1000
DAP	U	3.8×10^{-4}	1.0 ± 0.08	460
AP	C	ND	1.5 ± 0.1	450
AP	U	ND	2.2 ± 0.1	330

[a] Folding data are presented for FRET analysis of the BA vectors. Hill coefficients and $[Mg^{2+}]_{1/2}$ values were derived by fitting FRET efficiencies for end-to-end vectors to a two-state folding model. The errors reported for the Hill coefficients are the asymptotic standard errors. Cleavage rate constants are the mean of three determinations of cleavage rates under single-turnover conditions at 25 °C. ND, not determined.

essentially inactive, and that folding is similar to that of a loop-free junction (*33*). In the NMR structure of isolated loop A (*49*), A9 makes a sheared base pairing interaction with G+1. Burke and colleagues (*50*) have proposed that the active form of the ribozyme requires the formation of a triple interaction between A9, G+1, and C25, whereby C25 forms a Watson−Crick interaction with G+1 (Figure 6). We have therefore made changes in base and functional groups at the +1 and 25 positions (retaining adenine at the 9 position throughout), investigating the folding and activity of the ribozyme in the context of the four-way helical junction. The results are summarized in Table 3.

Effects of Base Substitutions. We have shown previously (*33*) that the single-base change G+1A results in severely impaired folding of the junction form of the ribozyme. This is manifest in both a lowered affinity for magnesium ions ($[Mg^{2+}]_{1/2}$ = 650 μM, compared to <50 μM for the natural sequence) and a lower cooperativity of binding (n = 1.0, compared to 2 for the natural sequence). The cleavage activity of this species is also impaired, the rate being reduced by more than 1000-fold relative to that of the natural sequence (k_{rel} = 0.0009).

We have also investigated the single-base change C25U, which has similar properties (Figure 7A). Both folding ($[Mg^{2+}]_{1/2}$ = 940 μM and n = 0.9 ± 0.04) and cleavage activity (k_{rel} = 0.004) were impaired. Pinard et al. (*50*)

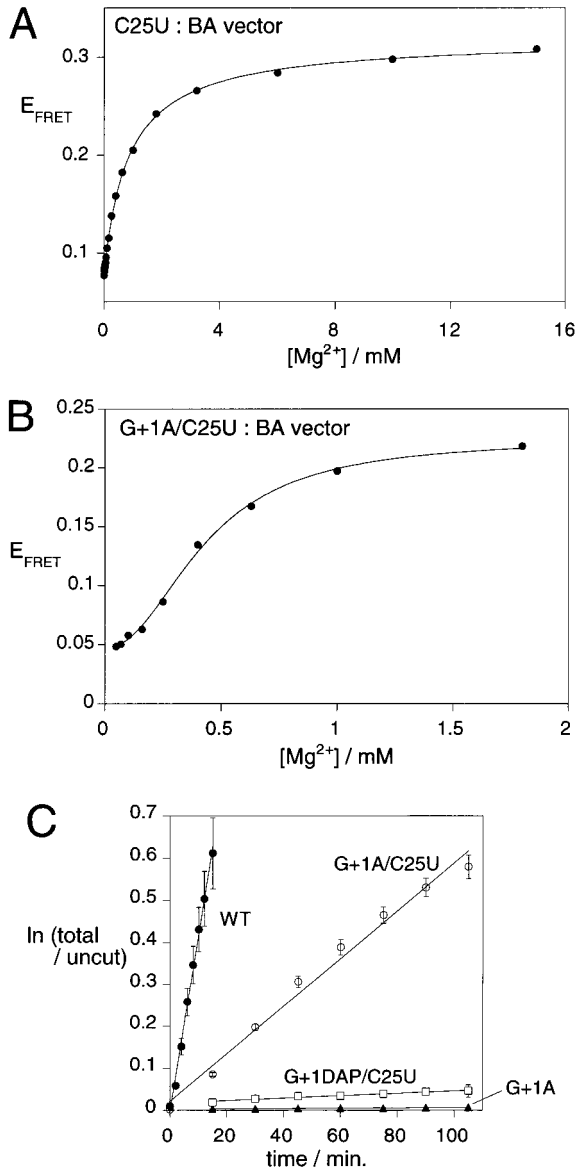

FIGURE 7: Ion-induced folding of hairpin ribozyme sequence variants based on C25U. (A) Plot of FRET efficiency as a function of magnesium ion concentration in the range of 0−16 mM for the BA vector of the C25U ribozyme (●). The data have been fitted by regression to the two-state model (line). The shape of the magnesium ion dependence indicates noncooperative behavior. (B)-Plot of FRET efficiency as a function of magnesium ion concentration in the range of 0−2 mM for the BA vector of the G+1A/C25U ribozyme (●). The data have been fitted by regression to the two-state model (line). In contrast to the C25U variant, the shape of the magnesium ion dependence is clearly cooperative. (C) Cleavage reaction progress for ribozyme variants. Ribozyme and radioactively labeled substrate strands (natural sequence and variants) were incubated in the presence of 10 mM magnesium ions at 25 °C, and aliquots were removed at various times. Products were separated by polyacrylamide gel electrophoresis, and quantified by phosphorimaging. The data are plotted in semilogarithmic form, from which rate constants were calculated. The data points are averages of triplicate measurements, and the errors are standard deviations: (●) natural sequence, (▲) G+1A, (○) G+1A/C25U, and (□) G+1DAP/C25U.

showed that the double mutation G+1A/C25U significantly restored the cleavage activity of the hinged form of the ribozyme. We made the same G+1A/C25U variant of the junction form of the ribozyme, and found that the two changes were compensatory to a significant degree in both

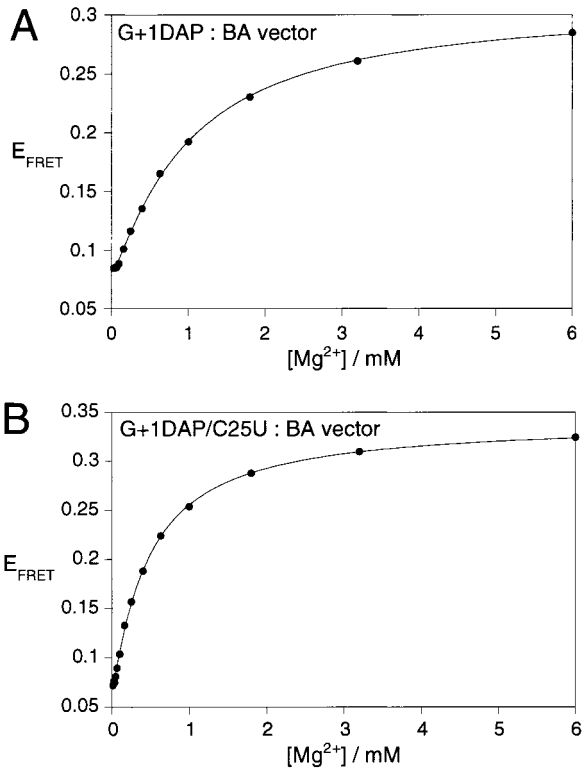

FIGURE 8: Ion-induced folding of hairpin ribozyme sequence variants based on 2,6-diaminopurine substitution at the +1 position. (A) Plot of FRET efficiency as a function of magnesium ion concentration in the range of 0−6 mM for the BA vector of the G+1DAP ribozyme (●). The data have been fitted by regression to the two-state model (line). The shape of the magnesium ion dependence indicates noncooperative behavior. (B) Plot of FRET efficiency as a function of magnesium ion concentration in the range of 0−6 mM for the BA vector of the G+1DAP/C25U ribozyme (●). The data have been fitted by regression to the two-state model (line). The shape of the magnesium ion dependence remains noncooperative despite the double substitution.

folding and cleavage activity (Figure 7B). The cooperativity of magnesium ion binding was fully restored ($n = 2.1 \pm 0.2$), although the affinity was reduced by an order of magnitude compared to that of the natural sequence ($[Mg^{2+}]_{1/2} = 431\ \mu M$). The rate of cleavage was substantially higher than the value of either of the single-base variants alone, but still below that of the natural-sequence ribozyme ($k_{rel} = 0.12$) (Figure 7C).

Effects of Functional Group Modifications. Chowrira et al. (*32*) showed that a hinged hairpin ribozyme in which the guanine at position +1 was replaced with inosine was essentially inactive, suggesting an important role for the exocyclic amine at position 2. This would be consistent with the proposed A9−G+1−C25 triple interaction. We reasoned that replacing G+1 with 2,6-diaminopurine (DAP) should weaken the triple interaction, removing two hydrogen bonds with cytosine (donated by N_4 and accepted by N_3 of cytosine). However, if a second change were made, replacing C25 with uridine, the resulting A9−DAP+1−U25 triple interaction should be closely similar in structure and stability to the proposed A9−G+1−C25 interaction (Figure 6).

The single-base change G+1DAP resulted in a reduced level of folding and a reduced cleavage rate. Magnesium ion binding was essentially noncooperative ($n = 1.1 \pm 0.05$), and the affinity was relatively weak ($[Mg^{2+}]_{1/2} = 1.0$ mM) (Figure 8A). Cleavage rates were also reduced ($k_{rel} = 0.004$).

The effects of the G+1DAP change were partially compensated by the C25U change. Magnesium ion binding in the double variant G+1DAP/C25U remained noncooperative ($n = 1.0 \pm 0.08$) (Figure 8B), and while the apparent magnesium ion affinity and the cleavage rate were elevated a little compared to those of the single-base variant G+1DAP, both parameters were much closer to the values of the single-base variant than those of the natural-sequence ribozyme, with a $[Mg^{2+}]_{1/2}$ of 460 μM and a k_{rel} of 0.008 (Figure 7C).

We have also investigated replacing G+1 with 2-aminopurine (AP). This base retains the exocyclic amino substituent at C_2, but lacks the carbonyl oxygen atom at C_6. This could form one fewer hydrogen bond in the interaction with a uridine base at position 25, but otherwise, it should be a relatively minor change from DAP in the context of the proposed triple interaction. Unfortunately, it was necessary to introduce 2-aminopurine as a 2′-deoxynucleotide. This variation was investigated in combination with both cytosine and uridine at position 25. Interestingly, in both cases the magnesium ion binding was cooperative, and reached the level of the natural ribozyme for the double variant G+1AP/C25U with a Hill coefficient n of 2.2 ± 0.1. The apparent affinities were relatively high in both cases ($[Mg^{2+}]_{1/2} = 450$ and 330 μM for the single- and double-base variants, respectively), although these values remain an order of magnitude weaker than that of the natural-sequence ribozyme. We have not investigated cleavage rates in these variants.

DISCUSSION

We have analyzed the folding of hairpin ribozyme variants using the change in efficiency of FRET between fluorophores terminally attached to helical arms. For this purpose, the most informative end-to-end distances are those between helices A and B, and between helices C and D, since these undergo pronounced shortening during the folding process. The natural-sequence hairpin ribozyme exhibits a cooperative folding induced by the binding of metal ions, in the magnesium ion concentration range of 0−200 μM. The ribozyme undergoes a further folding step at a higher magnesium ion concentration that will be discussed in a forthcoming paper; here we study the initial transition that brings about the close loop−loop interaction with correspondingly short BA and DC vectors. Using a simple two-state model to fit the FRET data in this region, we analyze the folding in terms of the cooperativity of magnesium ion binding, characterized by the Hill coefficient (n), and the apparent affinity of binding, characterized by the calculated magnesium ion concentration at which the transition is half-complete ($[Mg^{2+}]_{1/2}$). The apparent association constant (K_A) will depend on the overall free energy of this transition ($\Delta G^\circ_{fold} = -RT \ln K_A$). Less stable folded forms of the RNA will therefore require a higher magnesium ion concentration to drive the equilibrium toward the folded conformation, since the fraction of folded RNA is dependent upon the magnitude of $(K_A[Mg^{2+}]^n)^{-1}$. The extreme cases are the natural-sequence ribozyme in its junction form, where $n \sim 2$ and $[Mg^{2+}]_{1/2} < 50$ μM, and its isolated junction (where the unpaired A and B loops have been removed by complementation), where $n = 1$ and $[Mg^{2+}]_{1/2} \sim 2.5$ mM. The assumption of a two-state model may be a simplification since it seems likely that the average unfolded conformation will be influenced by the magnesium ion concentration. However, the significant differences in both the affinity and cooperativity of magnesium binding by hairpin ribozyme variants allows for an unambiguous interpretation of the data, and renders the consideration of more complex models unnecessary.

The first point to note is that the folding of none of the various hairpin variants reverts to that of the simple junction, and none is totally inactive in ribozyme cleavage. Even severely impaired species such as G+1A, A10U, and C25U, where the cooperativity of ion binding is close to unity, become half-folded at magnesium ion concentrations that are significantly lower than that for the isolated junction species. Evidently, the modified loops continue to influence the folding process despite their altered sequences. This suggests that multiple interactions exist between the loops, so no single-base change is sufficient to prevent all favorable interaction. We can arrange the loop A sequence variants in the order of their affinity for magnesium ions: natural > G8U > A7U > A9U > A10U ~ G+1A. With the exception of G8U, which we discuss below, there is a qualitative correlation with the measured cleavage activity of these species. We observe a similar correlation between folding and cleavage activity in the 2′-deoxyribose-substituted forms of the hairpin ribozyme. These results demonstrate the importance of folding as a prerequisite for catalytic activity, and provide further physical evidence for the importance of the loop−loop interaction in generating the active form of the ribozyme.

The folding of A10U is severely affected, where $n = 0.9$ and $[Mg^{2+}]_{1/2} = 640$ μM. In the structure of the isolated loop A determined in solution by NMR (*49*), A10 forms a sheared base pair with a cytosine at the −1 position, requiring protonation of this adenine. The base at position −1 is an adenine in the natural satellite RNA, and the cleavage rate measured in the hinged form of the ribozyme is insensitive to sequence variation at this position (*39*). It is therefore likely that when the loops become juxtaposed, A10 makes contact elsewhere, and could well interact with loop B.

Further evidence for contact between A10 and loop B comes from the effect of removing 2′-hydroxyl groups from selected ribose moieties. In general, the influence of single-deoxyribose substitutions was found to be relatively small, consistent with the loop−loop contact resulting from a number of interactions, none of which is dominant. However, the order of magnesium ion affinities (natural > dA9 > dA10 > dC25 ~ dA10 plus dC25) is instructive. Deoxyribose substitution of A9 was not expected to have a major effect. The reduction in affinity may be due to a structural change induced by an altered sugar pucker. Deoxyribose substitution of A10 has a greater effect, but the double substitution of A10 and C25 has no greater effect than the single substitution of C25. Both the original ribose zipper proposal of Earnshaw et al. (*26*) and the revised proposal of Ryder and Strobel (*46*) involve hydrogen bonding between the 2′-hydroxyl groups of A10 and C25 (Figure 9). The redundancy of the A10 substitution when combined with the C25 substitution suggests that the 2′-hydroxyl of A10 only forms a single hydrogen bond with the 2′-hydroxyl of C25. The weaker affinity of the C25 2′-deoxyribose variant is consistent with the formation of a second hydrogen bond by the 2′-hydroxyl of C25. Thus, we believe that our data are consistent with

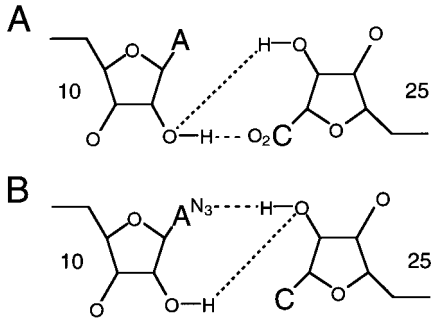

FIGURE 9: Proposed components of a ribose zipper. Schematic illustrating two proposals for ribose−ribose and ribose−base interactions between A10 and C25. (A) The proposal of Earnshaw et al. (*26*), in which the 2′-hydroxyl of A10 is hydrogen bonded to the 2′-hydroxyl and O_2 of C25. (B) The proposal of Ryder and Strobel (*46*), in which the 2′-hydroxyl of C25 is hydrogen bonded to the 2′-hydroxyl and N_3 of A10.

the proposal of Ryder and Strobel (*46*). The existence of a hydrogen bond in the active conformation involving the 2′-hydroxyl of A10 has been questioned (*48*). Our FRET efficiencies reflect the docked conformation, and it is possible that the proposed hydrogen bond contributes to loop−loop interaction but is broken in a subsequent conformational change forming the active state.

From molecular modeling, Burke and colleagues have proposed the existence of a triple interaction between A9, G+1, and C25 in the folded ribozyme (*50*) (Figure 6). They showed that cleavage activity in the hinged form of the ribozyme could be partially restored in the double variant G+1A/C25U; however, no folding was detected in the hinged ribozyme with this sequence. Previously, we have shown that the folding of the G+1A ribozyme variant in the junction form is significantly compromised (*33*). Here we find that replacement of the adenine at the 9 position by uridine (A9U) leads to rather small changes in the folding and cleavage activity of the junction form of the ribozyme compared to the natural sequence. In contrast, when the base of C25 was replaced with uridine, the activity of the resulting ribozyme in the junction form was significantly reduced (k_{rel} = 0.004), and folding was severely impaired (n = 0.9, $[Mg^{2+}]_{1/2}$ = 940 μM). Cleavage in the hinged form of the ribozyme was also found to be intolerant of substitution at this position (*17*), and a hinged C25U ribozyme failed to fold in high concentrations of magnesium or hexammine cobalt(III) ions (*50*). In the NMR structure of the isolated loop B (*51*), C25 makes a poorly defined interaction with U37, linked by a single hydrogen bond. However, U37 can be replaced with any other base with very little loss of cleavage activity in the hinged form of the ribozyme (*17*), and thus, the role of C25 in the complete ribozyme is likely to be in the formation of tertiary contacts.

The double change G+1A/C25U resulted in a significant recovery of ribozyme folding and cleavage activity in the junction form, although both were below the levels of the natural ribozyme, and this is good evidence for a Watson−Crick base pair between G+1 and C25 in the folded ribozyme. In the proposal of Burke and co-workers (*50*), A9 makes a further interaction on the minor groove edge of this base pair, generating the A9−G+1−C25 triple-base interaction shown in Figure 6. However, we note that substitution of A9 with uridine has a relatively small effect on folding and activity of the ribozyme. We investigated the double variant G+1DAP/C25U; this can potentially form the three-base A9−DAP+1−U25 interaction (Figure 6), which would be isosteric with that proposed for the natural sequence. While some restoration in folding and cleavage activity was observed compared to the two single-base variants, G+1DAP/C25U is less active than either G+1A/C25U or G+1AP/C25U (the latter can potentially form another three-base interaction isosteric with the proposed A9−G+1−C25 triple-base interaction, but with fewer hydrogen bonds). At present, we are unable to advance a unifying rationalization consistent with all the present data. For example, we note that the simultaneous presence of exocyclic amino groups at positions 2 and 6 of purine at position +1 results in folding that is significantly more impaired than when either alone is present. This may reflect a complex network of hydrogen bonding that will require a high-resolution three-dimensional structure for a full understanding. Overall, our results indicate an important role for the G+1·C25 base pair. This may be buttressed by an interaction with A9, but this is likely to play a more minor role, the loss of which has less significant consequences for folding.

In contrast to the simple four-way junction, the hairpin ribozyme in the junction form exhibits cooperativity in magnesium ion-induced folding (*28*). This is likely to result from the binding of one ion at the junction and one or more by the loops of the ribozyme. The observation of a loss of cooperativity in variant ribozymes implies that magnesium binding does not contribute to the stabilization of the loop−loop interaction in these species. The C25U, G+1A, and G+1DAP variants all exhibit noncooperative binding, and cooperativity is reduced for the G+1AP variant, indicating that G+1 and C25 are necessary for the productive binding of magnesium ions. The double variants G+1A/C25U and G+1AP/C25U restore cooperativity, but the variant G+1DAP/C25U does not. This suggests that the bases do not directly interact with magnesium but are essential to the creation of the conformational environment that is necessary for binding. The A10U variant also exhibits noncooperativity, implicating this base, at least indirectly, in magnesium binding. Interestingly, the 2′-deoxyribose substitution at C25 reduces cooperativity of binding. The loss of a hydrogen bond between the 2′-hydroxy of C25 and N_3 of A10 could result in a subtle conformational change at A10, reducing the affinity for magnesium. We believe these data further support the ribose zipper model of Ryder and Strobel (*46*).

For the majority of sequence changes to the junction form of the ribozyme, we have found a good correlation between the effects on folding and on cleavage activity. The major exception to this is the G8U variant. This species folds almost indistinguishably from the natural ribozyme (n = 2, $[Mg^{2+}]_{1/2}$ = 46 μM), but is very impaired in catalytic activity (k_{rel} = 0.009). Cleavage activity of the hinged form of the ribozyme is also highly intolerant of substitution at this position (*39*). It has been recently proposed that the guanine nucleobase at position 8 acts as a general base in the catalytic mechanism of the ribozyme (J. Burke, personal communication). Our results show that substitution of the guanine base at the 8 position has a major effect on cleavage activity, yet virtually none on folding. While not proving the role, these data are fully consistent with the proposed catalytic function of this base. We note that evidence is accumulating for nucleobase

catalysis by cytosine in the HDV ribozyme (*52*, *53*) and by adenine in the peptidyl transferase activity of the 23S rRNA (*5*, *54*).

A number of factors could contribute in principle to the observed rate enhancement of cleavage catalyzed by the hairpin ribozyme. These include conformational effects and the direct role of bound metal ions and nucleobases. RNA conformation will contribute to the rate enhancement for bond cleavage if the local geometry facilitates the trajectory into an in-line transition state for the transesterification reaction. Presumably, a conformational change during or after the interaction of loops A and B creates such a favorable local geometry, but this effect is unlikely to contribute a factor of more than 2 orders of magnitude to the overall observed rate enhancement. Metal ions are believed to be important in the small nucleolytic ribozymes, acting as either a Lewis acid to stabilize negative charge in the transition state or leaving group or in general base catalysis by their inner hydration sphere. However, in the case of the hairpin ribozyme, a direct role for metal ions has been called into question by the failure to observe a kinetic effect of phosphorothioate substitution at the scissile phosphate, and the demonstration that the reaction can proceed in the presence of hexammine cobalt(III) ions (*55*−*57*), or even in high concentrations of monovalent ions such as lithium or ammonium (*58*). On the basis of the evidence presented here, G8 is a clear candidate for nucleobase catalysis. For G8 to function as a general base, its pK_a would need to be perturbed by several units to bring it close to neutrality, which might occur in the environment of the folded ribozyme as the loops come into close interaction. However, if G8 does play a direct role in the chemistry of the cleavage reaction, it is not essential, because there is residual activity in the G8U ribozyme (Figure 2D); this variant is 4 times more active than the G+1A variant in the junction form of the ribozyme, for example. Thus, it is likely that catalysis of bond cleavage results from the combination of a number of processes, and no one factor is probably indispensable.

In summary, by investigating both the folding and activity of selected hairpin ribozyme variants, we have demonstrated the importance of magnesium binding to the folding process, and found evidence to support the revised ribose zipper model for docking interactions and the proposition that base pairing between G+1 and C25 is a significant factor in stabilizing loop−loop interactions. In addition, our data are consistent with the proposed catalytic function of G8.

ACKNOWLEDGMENT

We thank our colleagues Drs. Dan Lafontaine and Christian Hammann for discussion and Dr. J. Burke for discussion of unpublished data.

REFERENCES

1. Lilley, D. M. J. (1999) *Curr. Opin. Struct. Biol. 9*, 330−338.
2. Sigurdsson, S. T., Thomson, J. B., and Eckstein, F. (1998) *RNA structure and function*, pp 339−376, Cold Spring Harbor Laboratory Press, Plainview, NY.
3. Cech, T. R., and Herschlag, D. (1996) in *RNA catalysis* (Eckstein, F., and Lilley, D. M. J., Eds.) Vol. 10, pp 1−17, Springer-Verlag, Heidelberg, Germany.
4. Michel, F., and Ferat, J. L. (1995) *Annu. Rev. Biochem. 64*, 435−461.
5. Nissen, P., Hansen, J., Ban, N., Moore, P. B., and Steitz, T. A. (2000) *Science 289*, 920−930.
6. Woese, C. (1967) *The Genetic Code*, pp 179−195, Harper & Row, New York.
7. Orgel, L. E. (1986) *J. Theor. Biol. 123*, 127−149.
8. Fedor, M. J. (2000) *J. Mol. Biol. 297*, 269−291.
9. Buzayan, J. M., Gerlach, W. L., and Bruening, G. (1986) *Nature 323*, 349−353.
10. Feldstein, P. A., Buzayan, J. M., and Bruening, G. (1989) *Gene 82*, 53−61.
11. Hampel, A., and Tritz, R. (1989) *Biochemistry 28*, 4929−4933.
12. DeYoung, M. B., Siwkowski, A. M., Lian, Y., and Hampel, A. (1995) *Biochemistry 34*, 15785−15791.
13. van Tol, H., Buzayan, J. M., and Bruening, G. (1991) *J. Virol. 280*, 23−30.
14. Hegg, L. A., and Fedor, M. J. (1995) *Biochemistry 34*, 15813−15828.
15. Berzal-Herranz, A., Simpson, J., Chowrira, B. M., Butcher, S. E., and Burke, J. M. (1993) *EMBO J. 12*, 2567−2574.
16. Anderson, P., Monforte, J., Tritz, R., Nesbitt, S., Hearst, J., and Hampel, A. (1994) *Nucleic Acids Res. 22*, 1096−1100.
17. Siwkowski, A., Shippy, R., and Hampel, A. (1997) *Biochemistry 36*, 3930−3940.
18. Chowrira, B. M., Berzal-Herranz, A., Keller, C. F., and Burke, J. M. (1993) *J. Biol. Chem. 268*, 19458−19462.
19. Grasby, J. A., Mersmann, K., Singh, M., and Gait, M. J. (1995) *Biochemistry 34*, 4068−4076.
20. Schmidt, S., Beigelman, L., Karpeisky, A., Usman, N., Sorensen, U. S., and Gait, M. J. (1996) *Nucleic Acids Res. 24*, 573−581.
21. Komatsu, Y., Koizumi, M., Nakamura, H., and Ohtsuka, E. (1994) *J. Am. Chem. Soc. 116*, 3692−3696.
22. Butcher, S. E., Heckman, J. E., and Burke, J. M. (1995) *J. Biol. Chem. 270*, 29648−29651.
23. Komatsu, Y., Kanzaki, I., and Ohtsuka, E. (1996) *Biochemistry 35*, 9815−9820.
24. Komatsu, Y., Kanzaki, I., Shirai, M., and Ohtsuka, E. (1997) *Biochemistry 36*, 9935−9940.
25. Komatsu, Y., Shirai, M., Yamashita, S., and Ohtsuka, E. (1997) *Bioorg. Med. Chem. 5*, 1063−1069.
26. Earnshaw, D. J., Masquida, B., Müller, S., Sigurdsson, S. T., Eckstein, F., Westhof, E., and Gait, M. J. (1997) *J. Mol. Biol. 274*, 197−212.
27. Shin, C., Choi, J. N., Sang, S. I., Song, J. T., Ahn, J. H., Lee, J. S., and Choi, Y. D. (1996) *Nucleic Acids Res. 24*, 2685−2689.
28. Murchie, A. I. H., Thomson, J. B., Walter, F., and Lilley, D. M. J. (1998) *Mol. Cell 1*, 873−881.
29. Walter, F., Murchie, A. I. H., Thomson, J. B., and Lilley, D. M. J. (1998) *Biochemistry 37*, 14195−14203.
30. Walter, N. G., Hampel, K. J., Brown, K. M., and Burke, J. M. (1998) *EMBO J. 17*, 2378−2391.
31. Hampel, A., Tritz, R., Hicks, M., and Cruz, P. (1990) *Nucleic Acids Res. 18*, 299−304.
32. Chowrira, B. M., Berzal-Herranz, A., and Burke, J. M. (1991) *Nature 354*, 320−322.
33. Zhao, Z.-Y., Wilson, T. J., Maxwell, K., and Lilley, D. M. J. (2000) *RNA 6*, 1833−1846.
34. Walter, N. G., Burke, J. M., and Millar, D. P. (1999) *Nat. Struct. Biol. 6*, 544−549.
35. Fedor, M. J. (1999) *Biochemistry 38*, 11040−11050.
36. Bassi, G. S., Murchie, A. I. H., and Lilley, D. M. J. (1996) *RNA 2*, 756−768.
37. Bassi, G. S., Møllegaard, N. E., Murchie, A. I. H., and Lilley, D. M. J. (1999) *Biochemistry 38*, 3345−3354.
38. Bassi, G. S., Murchie, A. I. H., Walter, F., Clegg, R. M., and Lilley, D. M. J. (1997) *EMBO J. 16*, 7481−7489.
39. Shippy, R., Siwkowski, A., and Hampel, A. (1998) *Biochemistry 37*, 564−570.
40. Walter, F., Murchie, A. I. H., Duckett, D. R., and Lilley, D. M. J. (1998) *RNA 4*, 719−728.
41. Förster, T. (1948) *Ann. Phys. 2*, 55−75.

42. Murchie, A. I. H., Clegg, R. M., von Kitzing, E., Duckett, D. R., Diekmann, S., and Lilley, D. M. J. (1989) *Nature 341*, 763−766.
43. Clegg, R. M., Murchie, A. I. H., Zechel, A., Carlberg, C., Diekmann, S., and Lilley, D. M. J. (1992) *Biochemistry 31*, 4846−4856.
44. Clegg, R. M., Murchie, A. I. H., Zechel, A., and Lilley, D. M. J. (1993) *Proc. Natl. Acad. Sci. U.S.A. 90*, 2994−2998.
45. Norman, D. G., Grainger, R. J., Uhrin, D., and Lilley, D. M. J. (2000) *Biochemistry 39*, 6317−6324.
46. Ryder, S. P., and Strobel, S. A. (1999) *J. Mol. Biol. 291*, 295−311.
47. Cate, J. H., Gooding, A. R., Podell, E., Zhou, K. H., Golden, B. L., Kundrot, C. E., Cech, T. R., and Doudna, J. A. (1996) *Science 273*, 1678−1685.
48. Earnshaw, D. J., Hamm, M. L., Piccirilli, J. A., Karpeisky, A., Beigelman, L., Ross, B. S., Manoharan, M., and Gait, M. J. (2000) *Biochemistry 39*, 6410−6421.
49. Cai, Z. P., and Tinoco, I. (1996) *Biochemistry 35*, 6026−6036.
50. Pinard, R., Lambert, D., Walter, N. G., Heckman, J. E., Major, F., and Burke, J. M. (1999) *Biochemistry 38*, 16035−16039.
51. Butcher, S. E., Allain, F. H., and Feigon, J. (1999) *Nat. Struct. Biol. 6*, 212−216.
52. Perrotta, A. T., Shih, I., and Been, M. D. (1999) *Science 286*, 123−126.
53. Nakano, S., Chadalavada, D. M., and Bevilacqua, P. C. (2000) *Science 287*, 1493−1497.
54. Muth, G. W., Ortoleva-Donnelly, L., and Strobel, S. A. (2000) *Science 289*, 947−950.
55. Nesbitt, S., Hegg, L. A., and Fedor, M. J. (1997) *Chem. Biol. 4*, 619−630.
56. Hampel, A., and Cowan, J. A. (1997) *Chem. Biol. 4*, 513−517.
57. Young, K. J., Gill, F., and Grasby, J. A. (1997) *Nucleic Acids Res. 25*, 3760−3766.
58. Murray, J. B., Seyhan, A. A., Walter, N. G., Burke, J. M., and Scott, W. G. (1998) *Chem. Biol. 5*, 587−595.
59. Beaucage, S. L., and Caruthers, M. H. (1981) *Tetrahedron Lett. 22*, 1859−1862.
60. Hakimelahi, G. H., Proba, Z. A., and Ogilvie, K. K. (1981) *Tetrahedron Lett. 22*, 5243−5246.
61. Perreault, J.-P., Wu, T., Cousineau, B., Ogilvie, K. K., and Cedergren, R. (1990) *Nature 344*, 565−567.
62. Milligan, J. F., Groebe, D. R., Witherall, G. W., and Uhlenbeck, O. C. (1987) *Nucleic Acids Res. 15*, 8783−8798.
63. Clegg, R. M. (1992) *Methods Enzymol. 211*, 353−388.
64. Walter, F., Murchie, A. I. H., and Lilley, D. M. J. (1998) *Biochemistry 37*, 17629−17636.

BI002644P